Available online at www.sciencedirect.com
SCIENCE DIRECT®
ELSEVIER
Journal of Sound and Vibration 276 (2004) 755–780
JOURNAL OF SOUND AND VIBRATION
www.elsevier.com/locate/jsvi

A method for calculating the axisymmetric response of a two-layered half-space under dynamic concentrated loading

Q. Grimal, S. Naïli*, A. Watzky

Laboratoire de Mécanique Physique, CNRS UMR 7052 B2OA, Faculté des Sciences et Technologie, Université Paris XII-Val de Marne, 61, Avenue du Général de Gaulle, Créteil Cédex 94010, France

Received 10 March 2003; accepted 5 August 2003

Abstract

The transient response of a linearly elastic structure made of a layer overlaying a half-space, subjected to a normal point force on its free surface, is investigated. Both welded contact and frictionless sliding are considered at the interface. This paper presents a method to calculate the response, for a wide range of loading durations (T), on the axis of symmetry of the configuration (in the layer and the half-space). Equations of the boundary–value problem are manipulated in an integral transform domain and the Cagniard–de Hoop method is used. The final form of the exact analytical solution is a sum of contributions corresponding to the rays of the generalized ray theory; little computational effort need be developed for evaluating each contribution. While this theory has only been used to obtain early-time responses, long-time responses—up to 30 times the transit time of P-waves in the layer—have been calculated for this study. This work was conducted to help characterize the stress transmitted in the human lung (half-space) when the thoracic wall (layer) is subjected to a non-penetrating impact. Depending on T, multiple reflections of waves in the layer or typical low-frequency response are observed. The influence of the contact condition with respect to T is elucidated.

1. Introduction

The investigation presented in this paper arose out of the need for a better understanding of the transmission of mechanical energy within a layered structure subjected to a non-penetrating impact on its surface. In order to assess damage due to dynamic loading, both amplitudes and time histories of stresses and displacements may be relevant. In many cases when the structure can

*Corresponding author. Tel.: +33-1-45-17-1446; fax: +33-1-45-17-1433.
E-mail addresses: grimal@univ-paris12.fr (Q. Grimal), naili@univ-paris12.fr (S. Naïli), watzky@univ-paris12.fr (A. Watzky).

0022-460X/$ - see front matter © 2003 Elsevier Ltd. All rights reserved.
doi:10.1016/j.jsv.2003.08.037

be modelled as a stack of linearly elastic materials, analytical methods can be considered and histories obtained with great accuracy and little computational effort in a form that often yields much physical insight (as opposed to purely numerical methods like boundary or finite elements methods).

Mencher [1] investigated the simplest layered medium: a plate of infinite extent. He set the basis of a method that eventually yields exact analytical solutions for displacements and stresses under concentrated dynamic loading. Mencher obtained closed form solutions for the epicentral displacement, due to a buried source of pressure waves, as a sum of terms each corresponding to a wave reflected a certain number of times on the plate surfaces; this type of solution has later been referred to as a generalized ray solution [2], (see Ref. [3] for a review of the generalized ray theory) and is in general associated with the Cagniard–de Hoop method [4,5]. Following Mencher's work, many authors have contributed to the field by developing new solutions for the response at any receiver location and for various types of concentrated loadings in both axisymmetric [6–9] and non-axisymmetric [10,3,11] configurations.

In parallel with the method of solution for the calculation of the plate response, methods based on the generalized ray theory were developed for geophysical applications to compute synthetic seismograms in layered media with an arbitrary number of parallel layers (see Refs. [12,13] for reviews of the method). A typical generalized ray solution is not obtained straightforwardly by solving the elastodynamics equations with given boundary conditions but is constructed by intuition: the generalized rays to take into account are numbered and the analytic expression for the contribution of each ray is built by assembling different blocks—terms of a product—which stand for the type of source, the polarization of the wave at the receiver and at the source and coefficients of reflection/transmission. Doing so, many problems of wave propagation in stratified media can be treated without explicitly solving the tedious boundary–value problem.

In the most general cases—tridimensional configuration and arbitrary receiver location—each generalized ray contribution has an analytic expression that is not obtained in closed form and their evaluation requires some numerical computations. As a consequence, numerical results with the generalized ray theory have only been obtained in situations where a few number of rays need to be taken into account. In the generalized ray theory, the rays combine into ray groups [3], each of which contains all the rays that have undergone a given number of interactions—reflections and transmissions—with interfaces of the layered medium. In a plate excited by a point force on one of its surfaces, the number of rays in a group is 2^{n+1}, where n is the number of interactions of the rays with surfaces; in a layered medium, the number of rays is even more important since each wave that hits an interface gives rise to two reflected and two transmitted waves.

The complexity in the form of the solution for each ray is minimum for axisymmetric configurations where the receiver and the source are placed on the axis of symmetry; in such cases, exact analytical closed-form solutions can be derived in a *plate*. In the same source/receiver configuration in *layered media*, only one equation (the solution of which is the Cagniard contour) must be solved with a numerical method at each time instant, so that accurate solutions are obtained with little computational effort [14]. For arbitrary receiver and source locations, the generalized ray method is much more costly with respect to numerical computations because an integral must be evaluated for each ray; furthermore, since the contributions of head waves and surface waves must be calculated individually (and added to body waves contributions), the method must be implemented very cautiously. With receivers and source on the axis of symmetry,

head waves never contribute; and interface waves need only be computed for receivers on the interfaces.

In the present paper, the response of an elastic structure made of a layer overlaying a half-space and subjected to a time-dependent normal point force on the free surface is investigated (see Fig. 1)—this configuration is axisymmetric. Two contact conditions are considered at the interface: welded contact and frictionless sliding contact. The paper is focussed on the special case where the receiver is placed on the axis of symmetry (in the context of assessing the energy of impact transmitted in the half-space, these locations are those where maximum amplitudes are expected).

The aim of this paper is to present a method to obtain the *exact* solution of the elastodynamics problem for a wide range of loading durations. The results presented demonstrate that the response to relatively "*long*" *impulses*—of duration about 30 transit times of *P*-waves in the layer—can be calculated in practice with little computational effort by using the generalized ray theory. The low computational cost of each ray contribution in the configuration considered makes it possible to handle the several millions of rays required to obtain long-time responses. The algorithm of the calculation code is made efficient by generating the rays systematically by an iterative process.

In this paper, the derivation of the solution is constructed from the elastodynamics equations and the boundary conditions by using a matrix formulation. Doing so, the generalized ray decomposition of the solution is obtained as a result and not by intuition. This method has become popular recently [15–18]. Analytical solutions are derived in a Laplace–Fourier transform domain which is the dual of the time–space domain, and the inverse transformation for each ray contribution is performed by means of the Cagniard–de Hoop method. Even though in the present paper results are only given for receivers on the axis of symmetry of the configuration, the methodology—except for some details of the inverse transformation procedure—and the computational scheme presented are valid in the general case.

The response of a layered structure subjected to dynamic loading depends both on the relative stiffness of the materials and the duration of the loading. The response to a "short" impulse can be described in terms of waves while for a "long" impulse the characteristic dimensions of the

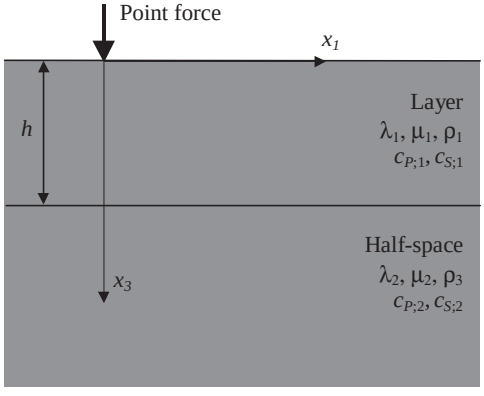

Fig. 1. Model configuration and co-ordinate system.

structure play a major role. For the structure considered in this paper (Fig. 1), a possible criterion for determining a priori the relative importance of wave versus structural phenomena is the ratio of the duration of the impulse with the transit time of a wave to cross the layer thickness once. If the ratio is far from one, then approximate theories may be considered; the method of solution presented, which is free of approximation, is especially useful in cases where the ratio is close to one—i.e., when the wavelengths involved are of the order of magnitude of the characteristic dimensions. As the method yields an exact solution of the elastodynamics problem, long-time, static values (obtained after equilibrium, when the structure has come back to rest) are obtained, even though the solution is expressed in terms of waves propagating.

The analysis presented in this paper was motivated by interest in the response of the human thorax subjected to a short pressure impulse, as, for instance, when a bullet is stopped by a bulletproof jacket. In this context, the layer and half-space correspond, respectively, to the thoracic wall and the lung. Since for the specific wave propagation problem under consideration there is no quantitative data available on the possible viscous mechanisms of energy dissipation in biological tissues, these mechanisms are not taken into account in the material models. However, viscous dissipation may somewhat modify the conclusions of this paper relative to the propagation of energy in the thorax model. The present work is a continuation of the work presented in Refs. [14,19], which dealt with similar model configurations and the same method of solution, but in which only the contribution of the first group of generalized rays transmitted in the half-space was considered. With the results presented in this paper, some mechanisms of the transmission of energy in the lung are elucidated.

Note that the method presented can be used for any set of values for the elastic properties of the layer and half-space. Typical engineering applications are found in non-destructive evaluation of materials.

The present paper is organized as follows: with this introduction as background, Section 2 gives a description of the configuration and the basic equations. In Section 3 the exact solution in a Laplace–Fourier domain is obtained as a sum of generalized ray contributions by using a matrix formulation. The transformation of each ray contribution back to the time–space domain is briefly presented in Section 4. Section 5 is devoted to the implementation of the method. In Section 6 the results of some computations for a material configuration and loading durations relevant to our biomechanical application are collected.

2. Description of the configuration and formulation of the problem

2.1. Configuration and definitions

Consider the structure represented in Fig. 1. It consists of a layer of infinite extent (medium 1) with thickness h overlaying a half-space (medium 2). The layer has a free surface, referred to as surface I, and the interface with the half-space is referred to as surface II. At surface II, the contact condition is, alternatively, perfect bonding (welded contact) or perfect sliding (smooth contact). Both media are linearly elastic, homogeneous and isotropic; for the characterization of the elastic properties, the Lamé constants λ and μ are used. The

mass density is denoted by ρ. Throughout this paper, superscripts (1) and (2) refer to media 1 and 2, respectively; however, superscripts may be omitted in equations valid for both media, if no ambiguity results.

The position is specified through the co-ordinates (x_1, x_2, x_3) with respect to a Cartesian reference frame $\mathscr{R}(O; \mathbf{x_1}, \mathbf{x_2}, \mathbf{x_3})$ where O is the origin and $(\mathbf{x_1}, \mathbf{x_2}, \mathbf{x_3})$ is an orthonormal basis for the space; the $\mathbf{x_3}$-axis is taken perpendicular to surfaces I and II. The free surface of the layer coincides with plane $x_3 = 0$ and the structure is localized in the half-space $x_3 \geqslant 0$. Time is denoted by t. The elastic response is characterized in $\mathscr{R}$ by the components σ_{ij} of the Cauchy stress tensor and by the components v_i of the particle velocity $\mathbf{v}$.

At the origin of the Cartesian reference frame (i.e., on the free surface), the layer is subjected to a dynamic point force of direction $\mathbf{x_3}$; hence both pressure (longitudinal) waves and shear (transverse) waves with vertical polarization are induced in the structure. Shear waves with horizontal polarization are not propagated in the configuration considered; however, the method of solution may be used with a point force of arbitrary direction, hence the formalism used in the sections to follow includes the possibility of dealing with shear waves of horizontal polarization.

Pressure and shear waves are denoted P- and S-waves, respectively; in the rest of the paper letters P and S are used for quantities relative to P- and S-waves, and each time a comma appears between P and S means that the quantities relative to P- or S-waves, respectively, must be used. Wave speeds are defined by $c_P = \sqrt{(\lambda + 2\mu)/\rho}$ and $c_S = \sqrt{\mu/\rho}$, and wave slownesses by $s_{P,S} = 1/c_{P,S}$. Media are at rest for $t < 0$.

Throughout the paper, the following notation convention is used (unless otherwise specified): vectors are typed bold upright; matrices are typed bold upright or black-board boldface upright (e.g., $\mathbb{D}$).

2.2. Governing equations, boundary and initial conditions

The equation of motion in the structure is

$$\partial_j \sigma_{ij} - \rho \partial_t v_i = 0, \quad i,j = 1,2,3, \tag{1}$$

where ∂_j and ∂_t denote, respectively, partial derivatives with respect to x_j and to time, δ_{ij} is the Kronecker symbol and Einstein's summation convention is used. The time derivative of Hooke's constitutive law for an elastic isotropic medium is introduced as

$$\partial_t \sigma_{ij} - \lambda \delta_{ij} \delta_{pq} \partial_q v_p - \mu(\partial_i v_j + \partial_j v_i) = 0. \tag{2}$$

Boundary conditions at the free surface: At surface I (plane $x_3 = 0$), the free surface conditions and the definition of loading are associated with the equations

$$\sigma_{13}(x_1, x_2, 0, t) = \sigma_{23}(x_1, x_2, 0, t) = 0, \quad \sigma_{33}(x_1, x_2, 0, t) = \sigma_0 \phi(t) \delta(x_1) \delta(x_2), \tag{3}$$

where $\phi(t)$ describes the history of the loading (with $\phi(t) = 0$ for $t < 0$), σ_0 its strength and δ is the Dirac function.

Sliding interface: The boundary conditions associated with sliding frictionless contact at surface II (plane $x_3 = h$) are

$$\begin{aligned} &[\![v_3]\!] = 0, \quad [\![\sigma_{33}]\!] = 0, \\ &\sigma_{13}^{(1)}(x_1, x_2, h, t) = \sigma_{23}^{(1)}(x_1, x_2, h, t) = 0, \\ &\sigma_{13}^{(2)}(x_1, x_2, h, t) = \sigma_{23}^{(2)}(x_1, x_2, h, t) = 0, \end{aligned} \tag{4}$$

where $[\![.]\!]$ denotes the jump of a quantity across the interface.

Welded interface: The boundary conditions associated with welded contact at surface II are

$$[\![\sigma_{13}]\!] = [\![\sigma_{23}]\!] = [\![\sigma_{33}]\!] = 0 \quad \text{and} \quad [\![v_1]\!] = [\![v_2]\!] = [\![v_3]\!] = 0. \tag{5}$$

3. Solution in the transform domain

The first of the two main stages in the derivation of the solution of the elastodynamics problem as stated in Section 2 is described in this section. The subsequent steps yield a solution in a Laplace–Fourier domain in the form of an infinite sum of terms, where each term can be identified with a generalized ray wave constituent (or, shortly, a ray) of the generalized ray theory.

In the following, the derivation is only presented for welded contact condition at surface II; the derivation for sliding contact is similar.

Taking into account the time invariance of the configuration, the equations given in Section 2.2 are subjected to a one-sided Laplace transform with respect to time. As an example, the time–space domain particle velocity $v_i(\mathbf{x}, t)$ is transformed to its Laplace–space domain counterpart $\hat{v}_i(\mathbf{x}, p)$ according to

$$\hat{v}_j(\mathbf{x}, p) = \int_0^\infty \exp(-pt) v_j(\mathbf{x}, t)\, \mathrm{d}t,$$

where p is real and positive. Subsequently, the shift invariance of the configuration with respect to x_1 and x_2 is exploited by applying a two-dimensional Fourier transformation to the Laplace-transformed equations. The Laplace–Fourier domain counterpart or, shortly, the transform domain counterpart $\tilde{v}_j(k_1, k_2, x_3, p)$ of $v_j(\mathbf{x}, t)$ is

$$\tilde{v}_j(k_1, k_2, x_3, p) = \int_{-\infty}^{\infty} \int_{-\infty}^{\infty} \exp[\mathrm{i}p(k_1 x_1 + k_2 x_2)] \hat{v}_j \, \mathrm{d}x_1 \, \mathrm{d}x_2,$$

where pk_1 and pk_2 are the real Fourier transform parameters.

After elimination of the stresses σ_{11}, σ_{12} and σ_{22}, in the transform domain counterparts of (1) and (2), six transform domain unknown state quantities remain to represent the wave field in each medium; they are arranged into the "motion-stress" state vector $\tilde{\mathbf{b}} = (\tilde{v}_1, \tilde{v}_2, \tilde{v}_3, -\tilde{\sigma}_{13}, -\tilde{\sigma}_{23}, -\tilde{\sigma}_{33})^{\mathrm{T}}$ (here T means transpose operator). In both media, the differential equation for $\tilde{\mathbf{b}}$ takes the form [13]

$$\partial_3 \tilde{\mathbf{b}} = -p\mathbf{A}\tilde{\mathbf{b}}, \tag{6}$$

where $\mathbf{A}$ is a (6×6) matrix. Instead of solving (6) straightforwardly, it is convenient to introduce the linear transformation

$$\tilde{\mathbf{b}} = \mathbf{D}\bar{\mathbf{w}}, \tag{7}$$

where each column of matrix $\mathbf{D}$ is an eigenvector of matrix $\mathbf{A}$. The normalization and ordering of the eigenvectors is the same as in Ref. [13]. The six components of $\bar{\mathbf{w}}$, called the "wave vector", stand for six independent wave motions each specified by a polarization and a direction of propagation with respect to the $\mathbf{x}_3$-axis. For later use, $\bar{\mathbf{w}}$ is split in two parts

$$\bar{\mathbf{w}} = \begin{pmatrix} \bar{\mathbf{w}}^- \\ \bar{\mathbf{w}}^+ \end{pmatrix}, \quad \bar{\mathbf{w}}^- = (\bar{w}_1, \bar{w}_2, \bar{w}_3)^{\mathrm{T}}, \quad \bar{\mathbf{w}}^+ = (\bar{w}_4, \bar{w}_5, \bar{w}_6)^{\mathrm{T}},$$

where $\bar{\mathbf{w}}^-$ is associated with up-going waves (direction of decreasing x_3) and $\bar{\mathbf{w}}^+$ with down-going waves (direction of increasing x_3); $\bar{w}_1$ and $\bar{w}_4$ represent amplitudes of P-waves, $\bar{w}_2$ and $\bar{w}_5$ of S-waves with vertical polarization and, finally, $\bar{w}_3$ and $\bar{w}_6$ of S-waves with horizontal polarization. The matrix $\mathbf{D}$ is partitioned in (3×3) sub-matrices defined by

$$\mathbf{D} = \begin{pmatrix} \mathbf{D}_1 & \mathbf{D}_2 \\ \mathbf{D}_3 & \mathbf{D}_4 \end{pmatrix},$$

where

$$\mathbf{D}_1 = \begin{pmatrix} \mathrm{i}c_P k_1 & \mathrm{i}c_S s_3^S k_1 S^{-1} & -\mathrm{i}k_2 S^{-1} \\ \mathrm{i}c_P k_2 & \mathrm{i}c_S s_3^S k_2 S^{-1} & \mathrm{i}k_1 S^{-1} \\ -c_P s_3^P & c_S S & 0 \end{pmatrix}, \quad \mathbf{D}_2 = \begin{pmatrix} \mathrm{i}c_P k_1 & -\mathrm{i}c_S s_3^S k_1 S^{-1} & -\mathrm{i}k_2 S^{-1} \\ \mathrm{i}c_P k_2 & -\mathrm{i}c_S s_3^S k_2 S^{-1} & \mathrm{i}k_1 S^{-1} \\ c_P s_3^P & c_S S & 0 \end{pmatrix},$$

$$\mathbf{D}_3 = \begin{pmatrix} -2\mu\mathrm{i}c_P s_3^P k_1 & -2\mu\mathrm{i}c_S \chi k_1 S^{-1} & \mu\mathrm{i}s_3^S k_2 S^{-1} \\ -2\mu\mathrm{i}c_P s_3^P k_2 & -2\mu\mathrm{i}c_S \chi k_2 S^{-1} & -\mu\mathrm{i}s_3^S k_1 S^{-1} \\ 2\mu c_P \chi & -2\mu S c_S s_3^S & 0 \end{pmatrix},$$

$$\mathbf{D}_4 = \begin{pmatrix} 2\mu\mathrm{i}c_P s_3^P k_1 & -2\mu\mathrm{i}c_S \chi k_1 S^{-1} & -\mu\mathrm{i}s_3^S k_2 S^{-1} \\ 2\mu\mathrm{i}c_P s_3^P k_2 & -2\mu\mathrm{i}c_S \chi k_2 S^{-1} & \mu\mathrm{i}s_3^S k_1 S^{-1} \\ 2\mu c_P \chi & 2\mu S c_S s_3^S & 0 \end{pmatrix},$$

where $S^2 = -(k_1^2 + k_2^2)$, $\chi = 0.5 s_S^2 - S^2$ and $s_3^{P,S} = (s_{P,S}^2 - S^2)^{1/2}$. In order to keep the square roots single valued in the derivations to follow, the complex quantities $s_3^{P,S}$ are chosen so that $\Re[s_3^{P,S}] \geqslant 0$, where $\Re[x]$ denotes the real part of x.

Substituting (7) into (6), the following differential equation for the wave vector is obtained

$$\partial_3 \bar{\mathbf{w}} = -p\mathbf{\Lambda}\bar{\mathbf{w}}, \tag{8}$$

where $\mathbf{\Lambda}$ is a diagonal matrix whose non-zero terms λ_i are the eigenvalues of $\mathbf{A}$ defined by [13]

$$\lambda_1 = -s_3^P, \quad \lambda_2 = -s_3^S, \quad \lambda_3 = -s_3^S, \quad \lambda_4 = s_3^P, \quad \lambda_5 = s_3^S, \quad \lambda_6 = s_3^S.$$

The six solutions of Eq. (8) have the structure of inhomogeneous plane waves propagating in direction $\mathbf{x_3}$

$$\bar{w}_n = w_n \exp(-p\lambda_n x_3). \tag{9}$$

Note the use of a bar to distinguish $\bar{w}_n$ from the term w_n in factor of the exponential. In parenthesis appears the phase of the transform domain wave. For quantities in medium 1, the

phase is chosen zero at surface I and for quantities in medium 2, the phase is chosen zero at surface II.

Solving the elastodynamics problem in the transform domain consists of determining $\tilde{\mathbf{b}}^{(1)}$ via $\bar{\mathbf{w}}^{(1)}$ in the layer and $\tilde{\mathbf{b}}^{(2)}$ via $\bar{\mathbf{w}}^{(2)}$ in the half-space (the solutions are coupled by the interface conditions). In medium 2, the three components of $\bar{\mathbf{w}}^{(2)-}$, which are associated with λ_n with negative real parts, are necessarily zero in order to satisfy the radiation condition (the amplitude must decrease when the distance with the source increases).

Until now, only the equations of motion have been used; the determination of the nine terms ($w_n^{(1)}$ and $w_n^{(2)}$) in factor of the exponential in Eq. (9) follows from a system of nine linear equations derived from the boundary conditions.

The transform domain counterpart of the boundary conditions at the free surface (3) is

$$\tilde{\sigma}_{i3}(k_1, k_2, 0, p) = \sigma_0 \hat{\phi}(p) \delta_{i3}, \quad i = 1..3, \tag{10}$$

where $\hat{\phi}(p)$ is the Laplace transform of $\phi(t)$. The action of the point force, expressed in Eq. (10), is stored in the following vector:

$$\boldsymbol{\sigma} = \begin{pmatrix} \check{\boldsymbol{\sigma}} \\ \check{\boldsymbol{\sigma}} \end{pmatrix} = (0, 0, \sigma_0 \hat{\phi}(p), 0, 0, 0)^{\mathrm{T}},$$

where $\check{\boldsymbol{\sigma}}$ and $\check{\boldsymbol{\sigma}}$ are vectors with three components. Upon introducing the expressions of the stresses as given by Eq. (7), relation (10) is rewritten

$$\mathbf{D}_3^{(1)} \mathbf{w}^{(1)-} + \mathbf{D}_4^{(1)} \mathbf{w}^{(1)+} = \check{\boldsymbol{\sigma}}. \tag{11}$$

(The bar over $\mathbf{w}^{(1)\pm}$ has been omitted because the phase is zero at the free surface.) The transform domain counterpart of the welded contact conditions (5) is

$$\tilde{v}_i^{(1)}(k_1, k_2, h, p) = \tilde{v}_i^{(2)}(k_1, k_2, h, p); \quad \tilde{\sigma}_{i3}^{(1)}(k_1, k_2, h, p) = \tilde{\sigma}_{i3}^{(2)}(k_1, k_2, h, p), \quad i = 1...3. \tag{12}$$

Upon introducing the expressions of the stresses and velocities as given by Eq. (7), relation (12) is rewritten

$$\begin{aligned} &\mathbf{D}_1^{(1)} \bar{\mathbf{w}}^{(1)-} + \mathbf{D}_2^{(1)} \bar{\mathbf{w}}^{(1)+} - \mathbf{D}_2^{(2)} \mathbf{w}^{(2)+} = 0, \\ &\mathbf{D}_3^{(1)} \bar{\mathbf{w}}^{(1)-} + \mathbf{D}_4^{(1)} \bar{\mathbf{w}}^{(1)+} - \mathbf{D}_4^{(2)} \mathbf{w}^{(2)+} = 0. \end{aligned} \tag{13}$$

(The bar over $\mathbf{w}^{(2)+}$ has been omitted because phase is zero at the interface.) Eqs. (11) and (13) combine to form a system of nine linear equations:

$$\begin{pmatrix} \mathbf{D}_3^{(1)} & \mathbf{D}_4^{(1)} & 0 \\ \mathbf{D}_1^{(1)} \mathbb{I}^- & \mathbf{D}_2^{(1)} \mathbb{I}^+ & -\mathbf{D}_2^{(2)} \\ \mathbf{D}_3^{(1)} \mathbb{I}^- & \mathbf{D}_4^{(1)} \mathbb{I}^+ & -\mathbf{D}_4^{(2)} \end{pmatrix} \begin{pmatrix} \mathbf{w}^{(1)-} \\ \mathbf{w}^{(1)+} \\ \mathbf{w}^{(2)+} \end{pmatrix} = \begin{pmatrix} \check{\boldsymbol{\sigma}} \\ 0 \\ 0 \end{pmatrix}, \tag{14}$$

where $\mathbb{I}^{\pm}$, which contain the exponential terms, are defined according to

$$\mathbf{D}_l^{(1)} \bar{\mathbf{w}}^{(1)-} = \mathbf{D}_l^{(1)} \mathbb{I}^- \mathbf{w}^{(1)-}, \quad l = 1, 3; \qquad \mathbf{D}_l^{(1)} \bar{\mathbf{w}}^{(1)+} = \mathbf{D}_l^{(1)} \mathbb{I}^+ \mathbf{w}^{(1)+}, \quad l = 2, 4, \tag{15}$$

that is,

$$\mathbb{I}^- = \begin{pmatrix} \exp(-p\lambda_1^{(1)}h) & 0 & 0 \\ 0 & \exp(-p\lambda_2^{(1)}h) & 0 \\ 0 & 0 & \exp(-p\lambda_3^{(1)}h) \end{pmatrix},$$

$$\mathbb{I}^+ = \begin{pmatrix} \exp(-p\lambda_4^{(1)}h) & 0 & 0 \\ 0 & \exp(-p\lambda_5^{(1)}h) & 0 \\ 0 & 0 & \exp(-p\lambda_6^{(1)}h) \end{pmatrix}.$$

3.1. Transform domain solution in the layer

Upon rewriting $\mathbf{w}^{(2)+}$ in terms of $\mathbf{w}^{(1)-}$ and $\mathbf{w}^{(1)+}$, relation (14) is rewritten as a system of six equations for $\mathbf{w}^{(1)}$

$$\begin{pmatrix} \mathbf{D}_3^{(1)} & \mathbf{D}_4^{(1)} \\ [\mathbf{D}_1^{(1)} - \mathbf{D}_2^{(2)}(\mathbf{D}_4^{(2)})^{-1}\mathbf{D}_3^{(1)}]\mathbb{I}^- & [\mathbf{D}_2^{(1)} - \mathbf{D}_2^{(2)}(\mathbf{D}_4^{(2)})^{-1}\mathbf{D}_4^{(1)}]\mathbb{I}^+ \end{pmatrix} \begin{pmatrix} \mathbf{w}^{(1)-} \\ \mathbf{w}^{(1)+} \end{pmatrix} = \boldsymbol{\sigma}.$$

Or in compact form

$$\mathbb{D}\mathbf{w}^{(1)} = \boldsymbol{\sigma}. \tag{16}$$

Assuming that $\mathbb{D}$ is non-singular, the solution of this equation can be formally expressed as

$$\mathbf{w}^{(1)} = \mathbb{D}^{-1}\boldsymbol{\sigma}. \tag{17}$$

The velocities and stresses in the time–space domain may, at this stage, be calculated from $\tilde{\mathbf{b}}^{(1)} = \mathbf{D}^{(1)}(\mathbb{D}^{-1}\boldsymbol{\sigma})$ by performing inverse Laplace and Fourier transformations; different methods (numerical methods, calculation of residues, etc.) may be used that only yield approximate solutions. In this study, an alternative procedure which makes use of the Cagniard–de Hoop method and yields exact solutions is used. The method requires an appropriate form of the transform domain solution to be derived from (17); in particular, all the terms where the Laplace transform parameter p occurs should be in the form $\exp[-pg(k_1, k_2, x_3)]$, where g is not function of p.

The subsequent derivation follows in essence the methodology presented by Ma and Lee [15] (see also Refs. [17,18]) for calculating the response of a plate of infinite extent subjected to a dynamic in-plane loading. Let the matrix $\mathbb{D}$ be split into two parts,

$$\mathbb{D} = \mathbb{G} + \mathbb{S},$$

with

$$\mathbb{G} = \begin{pmatrix} \mathbb{G}_1 & 0 \\ 0 & \mathbb{G}_2\mathbb{I}^+ \end{pmatrix}, \quad \mathbb{S} = \begin{pmatrix} 0 & \mathbb{S}_1 \\ \mathbb{S}_2\mathbb{I}^- & 0 \end{pmatrix},$$

where $\mathbb{G}_1$, $\mathbb{G}_2$, $\mathbb{S}_1$ and $\mathbb{S}_2$ are (3×3) matrices. Upon defining $\mathbf{R} = -\mathbb{S}^{-1}\mathbb{G}$, relation (17) takes the form

$$\mathbf{w}^{(1)} = (\mathbf{Id} - \mathbf{R})^{-1}\mathbb{S}^{-1}\boldsymbol{\sigma}, \tag{18}$$

where **Id** denotes the identity matrix. Finally, denoting $\mathbf{s} = \mathbb{S}^{-1}\boldsymbol{\sigma}$ and expanding matrix $(\mathbf{Id} - \mathbf{R})^{-1}$ into power series of **R**, relation (18) takes the form

$$\mathbf{w}^{(1)} = (\mathbf{Id} - \mathbf{R})^{-1}\mathbf{s} = \sum_{k=0}^{\infty} \mathbf{R}^k \mathbf{s}. \tag{19}$$

(See Ref. [16] for a discussion of the convergence of the sum in Eq. (19).) The components of **s** can be viewed as the amplitudes of the waves generated by the point force at the free surface. The vector **s** is split into two parts: $\mathbf{s} = (\check{\mathbf{s}}, \check{\mathbf{s}})^{\mathrm{T}}$, where $\check{\mathbf{s}}$ and $\check{\mathbf{s}}$ are vectors with three components defined by

$$\check{\mathbf{s}} = (0,0,0)^{\mathrm{T}}; \quad \check{\mathbf{s}} = \frac{\sigma_0 \hat{\phi}(p)}{2\mu_1 \Delta_{R;1}} (s_{P;1}\chi_1, s_{S;1}s_3^{P;1}S, 0)^{\mathrm{T}},$$

where $\Delta_{R;1} = s_3^{P;1}s_3^{S;1}S^2 + \chi_1^2$ is the "Rayleigh wave denominator". Noting that $(\mathbb{S}_2\mathbb{I}^-)^{-1}\mathbb{G}_2\mathbb{I}^+ = \mathbb{I}^+\mathbb{S}_2^{-1}\mathbb{G}_2\mathbb{I}^+$, matrix **R** may be written under the form

$$\mathbf{R} = \begin{pmatrix} 0 & \mathbb{I}^+\mathbf{R}_{\mathrm{II}}\mathbb{I}^+ \\ \mathbf{R}_{\mathrm{I}} & 0 \end{pmatrix}, \tag{20}$$

where $\mathbf{R}_{\mathrm{I}}$ and $\mathbf{R}_{\mathrm{II}}$ are three by three matrices given by

$$\mathbf{R}_{\mathrm{I}} = -\mathbb{S}_1^{-1}\mathbb{G}_1; \quad \mathbf{R}_{\mathrm{II}} = -\mathbb{S}_2^{-1}\mathbb{G}_2.$$

Matrix $\mathbf{R}_{\mathrm{I}}$ which only depends on the properties of medium 1, and matrix $\mathbf{R}_{\mathrm{II}}$, which depends both on the properties of media 1 and 2, are the well-known reflection coefficient matrices at surfaces I and II. Both have the following form:

$$\mathbf{R}_K = \begin{pmatrix} R_{PP}^K & R_{SP}^K & 0 \\ R_{PS}^K & R_{SS}^K & 0 \\ 0 & 0 & R_{SHSH}^K \end{pmatrix}, \quad K = \mathrm{I}, \mathrm{II},$$

where the subscript *SH* stands for *S*-waves with horizontal polarization. The coefficient $R_{\alpha\beta}^K$ is associated with an incident wave of polarization α reflected as a wave with polarization β. The calculated coefficients are given in Appendix A. The compact notation

$$\bar{\mathbf{R}}_{\mathrm{II}} = \mathbb{I}^+\mathbf{R}_{\mathrm{II}}\mathbb{I}^+ = -\begin{pmatrix} R_{PP}^{\mathrm{II}}\mathrm{e}^{-2p\lambda_4 h} & R_{SP}^{\mathrm{II}}\mathrm{e}^{-p(\lambda_4+\lambda_5)h} & 0 \\ R_{PS}^{\mathrm{II}}\mathrm{e}^{-p(\lambda_4+\lambda_5)h} & R_{SS}^{\mathrm{II}}\mathrm{e}^{-2p\lambda_5 h} & 0 \\ 0 & 0 & R_{SHSH}^{\mathrm{II}}\mathrm{e}^{-2p\lambda_5 h} \end{pmatrix}, \tag{21}$$

is used in the following (superscript "(1)" applies to all λ_n in Eq. (21)).

Giving the form of matrix **R** shown in Eq. (20), the power matrices $\mathbf{R}^k$ have specific forms for even and odd values of *k*

$$\mathbf{R}^k = \begin{pmatrix} (\bar{\mathbf{R}}_{\mathrm{II}}\mathbf{R}_{\mathrm{I}})^q & 0 \\ 0 & (\mathbf{R}_{\mathrm{I}}\bar{\mathbf{R}}_{\mathrm{II}})^q \end{pmatrix}, \quad k = 2q \ \forall q \in \mathcal{N},$$

$$\mathbf{R}^k = \begin{pmatrix} 0 & \bar{\mathbf{R}}_{\mathrm{II}}(\mathbf{R}_{\mathrm{I}}\bar{\mathbf{R}}_{\mathrm{II}})^q \\ \mathbf{R}_{\mathrm{I}}(\bar{\mathbf{R}}_{\mathrm{II}}\mathbf{R}_{\mathrm{I}})^q & 0 \end{pmatrix}, \quad k = 2q+1 \ \forall q \in \mathcal{N},$$

where $\mathcal{N}$ is the set of all natural numbers including 0.

Combining (7), (9) and (19), the final form of the transform domain solution is found to be

$$\tilde{b}_i^{(1)}(k_1,k_2,x_3,p)=\sum_{k=0}^{\infty}\sum_{n=1}^{6}D_{in}^{(1)}(\mathbf{R}^k\mathbf{s})_n\exp(-p\lambda_n^{(1)}x_3)=\sum_{k=0}^{\infty}\tilde{b}_{i;k}^{(1)}=\sum_{q=0}^{\infty}(\tilde{b}_{i;2q}^{(1)}+\tilde{b}_{i;2q+1}^{(1)}),\quad(22)$$

where $(.)_n$ (or $[.]_n$ in the following) denotes the nth-component of a vector and

$$\tilde{b}_{i;2q}^{(1)}=\sum_{n=4}^{6}D_{in}^{(1)}[(\mathbf{R}_{\mathrm{I}}\bar{\mathbf{R}}_{\mathrm{II}})^q\check{\mathbf{s}}]_n\exp(-p\lambda_n^{(1)}x_3)\quad\forall q\in\mathcal{N},$$

$$\tilde{b}_{i;2q+1}^{(1)}=\sum_{n=1}^{3}D_{in}^{(1)}[\bar{\mathbf{R}}_{\mathrm{II}}(\mathbf{R}_{\mathrm{I}}\bar{\mathbf{R}}_{\mathrm{II}})^q\check{\mathbf{s}}]_n\exp(-p\lambda_n^{(1)}x_3)\quad\forall q\in\mathcal{N}.\quad(23)$$

The form of solution (22) is identical to the solution obtained by intuition with the generalized ray method. Indeed, a component $\tilde{b}_i^{(1)}$ is basically a sum of many terms, each of which corresponds to a generalized ray. The amplitude of each term of the sum is the product of a component of the source vector $\mathbf{s}$ with reflection coefficients and a polarization term contained in matrix $\mathbf{D}$. The phase term associated with each ray, is a product of $\exp(-p\lambda_n^{(1)}x_3)$ with exponential terms, of the form $\exp(-p\lambda_n^{(1)}h)$, included in $\bar{\mathbf{R}}_{\mathrm{II}}$. The summation over n is the summation of the contributions of the waves of different polarizations arriving at the receiver. Each term of the sum over k is called a *ray group* and contains the contributions of rays which have been reflected k times on the layer boundaries. As can be seen from the sequences of reflection coefficients in (23), $\tilde{b}_{i;2q}^{(1)}$ and $\tilde{b}_{i;2q+1}^{(1)}$ are associated with down-going and up-going waves, respectively. As an example, the first three groups containing the rays which have been reflected zero, one and two times are detailed below:

$$\tilde{b}_{i;0}^{(1)}=D_{i4}s_4\mathrm{e}^{-ps_3^Px_3}+D_{i5}s_5\mathrm{e}^{-ps_3^Sx_3},$$

$$\begin{aligned}\tilde{b}_{i;1}^{(1)}=&D_{i4}R_{PP}^{\mathrm{II}}s_4\mathrm{e}^{-ps_3^P(2h-x_3)}+D_{i4}R_{SP}^{\mathrm{II}}s_5\mathrm{e}^{-p(s_3^P(h-x_3)+s_3^Sh)}\\&+D_{i5}R_{PS}^{\mathrm{II}}s_4\mathrm{e}^{-p(s_3^Ph+s_3^S(h-x_3))}+D_{i5}R_{SS}^{\mathrm{II}}s_5\mathrm{e}^{-ps_3^S(2h-x_3)},\end{aligned}$$

$$\begin{aligned}\tilde{b}_{i;2}^{(1)}=&D_{i4}R_{PP}^{\mathrm{I}}R_{PP}^{\mathrm{II}}s_4\mathrm{e}^{-ps_3^P(2h+x_3)}+D_{i4}R_{SP}^{\mathrm{I}}R_{PS}^{\mathrm{II}}s_4\mathrm{e}^{-p(s_3^P(h+x_3)+s_3^Sh)}\\&+D_{i4}R_{PP}^{\mathrm{I}}R_{SP}^{\mathrm{II}}s_5\mathrm{e}^{-p(s_3^P(h+x_3)+s_3^Sh)}+D_{i4}R_{SP}^{\mathrm{I}}R_{SS}^{\mathrm{II}}s_5\mathrm{e}^{-p(2s_3^Sh+s_3^Px_3)}\\&\times D_{i5}R_{PS}^{\mathrm{I}}R_{PP}^{\mathrm{II}}s_4\mathrm{e}^{-p(2s_3^Ph+s_3^Sx_3)}+D_{i5}R_{SS}^{\mathrm{I}}R_{PS}^{\mathrm{II}}s_4\mathrm{e}^{-p(s_3^Ph+s_3^{S:1}(h+x_3))}\\&+D_{i5}R_{PS}^{\mathrm{I}}R_{SP}^{\mathrm{II}}s_5\mathrm{e}^{-p(s_3^Ph+s_3^{S:1}(h+x_3))}+D_{i5}R_{SS}^{\mathrm{I}}R_{SS}^{\mathrm{II}}s_5\mathrm{e}^{-ps_3^S(2h+x_3)},\end{aligned}$$

where superscripts "(1)" have been omitted for quantities D_{in} and $s_3^{P,S}$. The ray group $\tilde{b}_{i;0}^{(1)}$ contains ray P and ray S which are the direct P- and S-waves arriving at the receiver (Lamb's problem for a half-space); the ray group $\tilde{b}_{i;1}^{(1)}$ contains the waves reflected once on surface II, rays PP, SP, PS and SS; the ray group $\tilde{b}_{i;2}^{(1)}$ contains the waves reflected once on surface II and once on surface I, PPP, PSP, SPP, SSP, PPS, PSS, SPS and SSS.

Denoting by $[\tilde{b}^{(1)}_{i;2q}]$ (resp. $[\tilde{b}^{(1)}_{i;2q+1}]$) the contribution of a single generalized ray to $\tilde{b}^{(1)}_{i;2q}$ (resp. $\tilde{b}^{(1)}_{i;2q+1}$), the symbolic forms of the rays are

$$[\tilde{b}^{(1)}_{i;2q}] = D^{(1)}_{in} \prod_{2q} R_{lm} s_r \exp\left[-p\left(\sum_{2q} s_3^{P,S} h + \lambda^{(1)}_n x_3\right)\right], \quad n = 4,5,6,$$

$$[\tilde{b}^{(1)}_{i;2q+1}] = D^{(1)}_{in} \prod_{2q+1} R_{lm} s_r \exp\left[-p\left(\sum_{2q+1} s_3^{P,S} h + \lambda^{(1)}_n x_3\right)\right], \quad n = 1,2,3, \tag{24}$$

where $\prod_N R_{lm}$ denotes the product of n *scalar* reflection coefficients, s_r denotes the amplitude of the wave generated at the source level, and subscript n is associated with the polarization at the receiver.

From a mathematical point of view, solution (24) is suited to the application of the Cagniard–de Hoop method because the Laplace parameter p only appears in the factor in the exponential.

3.2. Transform domain solution in the half-space

From (14), $\mathbf{w}^{(2)+}$ is rewritten in terms of $\mathbf{w}^{(1)+}$

$$\mathbf{w}^{(2)+} = \mathbf{T}_{\mathrm{II}} \bar{\mathbf{w}}^{(1)+},$$

where

$$\mathbf{T}_{\mathrm{II}} = [(\mathbf{D}^{(1)}_1)^{-1}\mathbf{D}^{(2)}_2 - (\mathbf{D}^{(1)}_3)^{-1}\mathbf{D}^{(2)}_4]^{-1}[(\mathbf{D}^{(1)}_1)^{-1}\mathbf{D}^{(1)}_2 - (\mathbf{D}^{(1)}_3)^{-1}\mathbf{D}^{(1)}_4].$$

The components of $\mathbf{T}_{\mathrm{II}}$ have exactly the same mathematical expressions as the transmission coefficients of plane waves and $\mathbf{T}_{\mathrm{II}}$ is the well-know transmission coefficient matrix of the form

$$\mathbf{T}_{\mathrm{II}} = \begin{pmatrix} T^{\mathrm{II}}_{PP} & T^{\mathrm{II}}_{SP} & 0 \\ T^{\mathrm{II}}_{PS} & T^{\mathrm{II}}_{SS} & 0 \\ 0 & 0 & T^{\mathrm{II}}_{SHSH} \end{pmatrix}.$$

Calculated expressions for the coefficients are given in Appendix A.

Given the solution $\tilde{b}_{i;2q}$ for down-going waves (associated with $\mathbf{w}^{(1)+}$) as expressed in Eq. (23), the transform-domain solution in the half-space is

$$\tilde{b}^{(2)}_i(k_1,k_2,x_3,p) = \sum_{q=0}^{\infty} \tilde{b}^{(2)}_{i;2q}, \tag{25}$$

where

$$\tilde{b}^{(2)}_{i;2q} = \sum_{n=4}^{6} D^{(2)}_{in}[\mathbf{T}_{\mathrm{II}}\mathbb{I}^{+}(\mathbf{R}_{\mathrm{I}}\bar{\mathbf{R}}_{\mathrm{II}})^q \check{\mathbf{s}}]_n \exp[-p\lambda^{(2)}_n(x_3 - h)]. \tag{26}$$

The form of solution (26) is identical to that obtained by intuition with the generalized ray method. The first two groups of transmitted waves are detailed below for illustration.

$$\begin{aligned}\tilde{b}^{(2)}_{i;0} = {} & D^{(2)}_{i4} T^{\mathrm{II}}_{PP} s_4 \mathrm{e}^{-p(s_3^{P;1}h + s_3^{P;2}(x_3-h))} + D^{(2)}_{i4} T^{\mathrm{II}}_{SP} s_5 \mathrm{e}^{-p(s_3^{S;1}h + s_3^{P;2}(x_3-h))} \\ & + D^{(2)}_{i5} T^{\mathrm{II}}_{PS} s_4 \mathrm{e}^{-p(s_3^{P;1}h + s_3^{S;2}(x_3-h))} + D^{(2)}_{i5} T^{\mathrm{II}}_{SS} s_5 \mathrm{e}^{-p(s_3^{S;1}h + s_3^{S;2}(x_3-h))},\end{aligned}$$

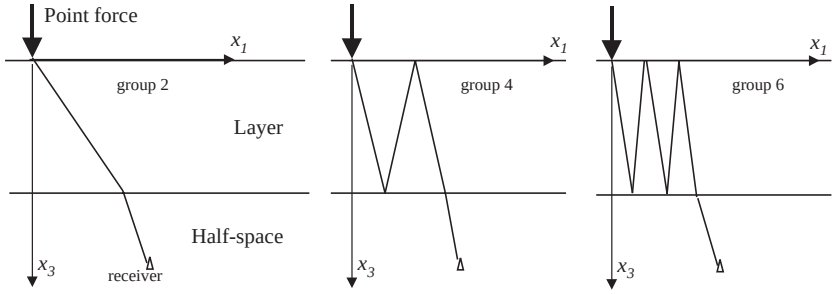

Fig. 2. Illustration of the ray groups. Only rays of type 2 (arriving in the half-space) are shown. Each ray is built with segments, where each segment represents a journey between surfaces I and II, or between a surface and the receiver (last segment). The group number is the number of segments of the rays of the group. Only one ray of each group is shown.

$$
\begin{aligned}
\tilde{b}^{(2)}_{i;2} = {} & D^{(2)}_{i4} T^{\mathrm{II}}_{PP} R^{\mathrm{I}}_{PP} R^{\mathrm{II}}_{PP} s_4 \mathrm{e}^{-p(3s_3^{P;1}h + s_3^{P;2}(x3-h))} + D^{(2)}_{i4} T^{\mathrm{II}}_{PP} R^{\mathrm{I}}_{SP} R^{\mathrm{II}}_{PS} s_4 \mathrm{e}^{-p(2s_3^{P;1}h + s_3^{S;1}h + s_3^{P;2}(x_3-h))} \\
& + D^{(2)}_{i4} T^{\mathrm{II}}_{PP} R^{\mathrm{I}}_{PP} R^{\mathrm{II}}_{SP} s_5 \mathrm{e}^{-p(2s_3^{P;1}h + s_3^{S;1}h + s_3^{P;2}(x_3-h))} + D^{(2)}_{i4} T^{\mathrm{II}}_{PP} R^{\mathrm{I}}_{SP} R^{\mathrm{II}}_{SS} s_5 \mathrm{e}^{-p(2s_3^{S;1}h + s_3^{P;1}h + s_3^{P;2}(x_3-h))} \\
& \times D^{(2)}_{i4} T^{\mathrm{II}}_{SP} R^{\mathrm{I}}_{PS} R^{\mathrm{II}}_{PP} s_4 \mathrm{e}^{-p(2s_3^{P;1}h + s_3^{S;1}h + s_3^{P;2}(x_3-h))} + D^{(2)}_{i4} T^{\mathrm{II}}_{SP} R^{\mathrm{I}}_{SS} R^{\mathrm{II}}_{PS} s_4 \mathrm{e}^{-p(s_3^{P;1}h + 2s_3^{S;1}h + s_3^{P;2}(x_3-h))} \\
& - D^{(2)}_{i4} T^{\mathrm{II}}_{SP} R^{\mathrm{I}}_{PS} R^{\mathrm{II}}_{SP} s_5 \mathrm{e}^{-p(s_3^{P;1}h + 2s_3^{S;1}h + s_3^{P;2}(x_3-h))} + D^{(2)}_{i4} T^{\mathrm{II}}_{SP} R^{\mathrm{I}}_{SS} R^{\mathrm{II}}_{SS} s_5 \mathrm{e}^{-p(3s_3^{S;1}h + s_3^{P;2}(x_3-h))} \\
& \times D^{(2)}_{i5} T^{\mathrm{II}}_{PS} R^{\mathrm{I}}_{PP} R^{\mathrm{II}}_{PP} s_4 \mathrm{e}^{-p(3s_3^{P;1}h + s_3^{S;2}(x3-h))} + D^{(2)}_{i5} T^{\mathrm{II}}_{PS} R^{\mathrm{I}}_{SP} R^{\mathrm{II}}_{PS} s_4 \mathrm{e}^{-p(2s_3^{P;1}h + s_3^{S;2}(x_3-h))} \\
& + D^{(2)}_{i5} T^{\mathrm{II}}_{PS} R^{\mathrm{I}}_{PP} R^{\mathrm{II}}_{SP} s_5 \mathrm{e}^{-p(2s_3^{P;1}h + s_3^{S;1}h + s_3^{S;2}(x_3-h))} + D^{(2)}_{i5} T^{\mathrm{II}}_{PS} R^{\mathrm{I}}_{SP} R^{\mathrm{II}}_{SS} s_5 \mathrm{e}^{-p(2s_3^{S;1}h + s_3^{P;1}h + s_3^{S;2}(x_3-h))} \\
& \times D^{(2)}_{i5} T^{\mathrm{II}}_{SS} R^{\mathrm{I}}_{PS} R^{\mathrm{II}}_{PP} s_4 \mathrm{e}^{-p(2s_3^{P;1}h + s_3^{S;1}h + s_3^{S;2}(x_3-h))} + D^{(2)}_{i5} T^{\mathrm{II}}_{SS} R^{\mathrm{I}}_{SS} R^{\mathrm{II}}_{PS} s_4 \mathrm{e}^{-p(s_3^{P;1}h + 2s_3^{S;1}h + s_3^{S;2}(x_3-h))} \\
& - D^{(2)}_{i5} T^{\mathrm{II}}_{SS} R^{\mathrm{I}}_{PS} R^{\mathrm{II}}_{SP} s_5 \mathrm{e}^{-p(s_3^{P;1}h + 2s_3^{S;1}h + s_3^{S;2}(x_3-h))} + D^{(2)}_{i5} T^{\mathrm{II}}_{SS} R^{\mathrm{I}}_{SS} R^{\mathrm{II}}_{SS} s_5 \mathrm{e}^{-p(3s_3^{S;1}h + s_3^{S;2}(x_3-h))}.
\end{aligned}
$$

An illustration of ray groups in the half-space is sketched in Fig. 2. The group $\tilde{b}^{(2)}_{i;2}$ is constructed from $\tilde{b}^{(1)}_{i;2}$, that is, each wave in $\tilde{b}^{(2)}_{i;2}$ is a wave of $\tilde{b}^{(1)}_{i;2}$ transmitted with P or S polarization. The series of terms of groups $\tilde{b}^{(2)}_{i;2q}$ can all be constructed systematically from (26).

Denoting by $[\tilde{b}^{(2)}_{i;2q}]$ the contribution of a single ray to $\tilde{b}^{(2)}_{i;2q}$, the symbolic form of the contribution of a ray is

$$
[\tilde{b}^{(2)}_{i;2q}] = D^{(2)}_{in} T^{\mathrm{II}}_{tn} \prod_{2q} R_{lm} s_r \exp\left[-p \left(\sum_{2q+1} s_3^{P,S} h + \lambda^{(2)}_n (x_3 - h) \right) \right], \quad n = 4, 5, 6, \tag{27}
$$

where T^{II}_{tn} is a transmission coefficient and the definition of the other quantities are the same as for (24). And, as before, from the mathematical point of view, Eq. (27) is suited to the application of the Cagniard–de Hoop method.

4. Solutions in the time–space domain

The second and last stage of the derivation of the solution of the problem stated in Section 2 is described in this section. The procedure described below yields the time–space counterpart for each term of the solution in form (24) and (27).

The solution for a single generalized ray contribution in layer (24) and in the half-space (27) is of the form

$$[\tilde{b}_i] = B_i(S)\exp[-pg(S)], \tag{28}$$

where

$$B_i(S) = D_{in}^{(1)} \prod_{2q} R_{lm} s_r \quad \text{(down-going ray in the layer)},$$

$$B_i(S) = D_{in}^{(1)} \prod_{2q+1} R_{lm} s_r \quad \text{(up-going ray in the layer)},$$

$$B_i(S) = D_{in}^{(2)} T_{tn}^{\mathrm{II}} \prod_{2q} R_{lm} s_r \quad \text{(down-going ray in the half-space)}.$$

The inverse Fourier transform of (28) is

$$[\hat{b}_i(\mathbf{x}, p)] = (p/2\pi)^2 \int_{-\infty}^{\infty} \int_{-\infty}^{\infty} B_i(S)\exp[-pg(S)]\,\mathrm{d}k_1\,\mathrm{d}k_2, \tag{29}$$

which is the Laplace transform of the time–space solution for a generalized ray contribution $[b_i(\mathbf{x}, t)]$. The Cagniard–de Hoop method is applied to (29). In essence, the method consists of changing the variable of integration and of deforming a contour of integration in the complex plane so that an equation—the Cagniard–de Hoop path of integration—of the form $g(S) = \tau$, where τ is real and positive, is satisfied (see Appendix B). Eventually, the inverse Laplace transform is found by inspection. The details of the derivation of the solution for a receiver located on the $\mathbf{x}_3$-axis were given in Ref. [14]; the final solution is

$$\begin{cases} [b_i(x_3, t)] = 0 & \text{for } t < T_a, \\ [b_i(x_3, t)] = -\dfrac{1}{2\pi}\partial_{tt}\phi(t) * \Re[B_i(S) S \partial_t S] & \text{for } t \geqslant T_a, \end{cases} \tag{30}$$

where T_a denotes the arrival time of the wave associated with the contribution (see Appendix B), time convolution is denoted by $*$, and S is solution of the Cagniard–de Hoop contour equation. The solution of the Cagniard–de Hoop contour for a receiver in the layer has an explicit analytic form (solution given in Appendix B); for a receiver in the half-space, the contour must be calculated with a numerical method of solution.

5. Numerical calculations

5.1. Computer program

A computer program has been developed based on the theory presented above. It mainly consists of (i) numbering and constructing all the rays arriving in a given time window, according to Eqs. (22) and (25) and by using the formula for the arrival times; (ii) calculating the time–space domain response for each ray according to Eq. (30) with $\partial_{tt}\phi(t) = \delta(t)$. For the purposes of numerical implementation, rays arriving at a receiver in the layer—rays of type 1—and rays arriving at a receiver in the half-space—rays of type 2—are treated separately. Eventually, all the

contributions are summed. The elastodynamic responses due to ray groups of increasing order are calculated successively, and independently. Note that the amplitude of each ray in a given group diverges with time while the sum of the amplitudes of all the rays in the group is convergent (this was first mentioned by Mencher [1]). The structure of the computer program is sketched in Fig. 3.

The number of rays in a group increases in powers of two with the number of segments: a group of rays with n segments contains 2^n rays.

Ray coding: The information on each ray is coded in a sequence of parameters. Sequences for rays of type 2 include: (i) the number of segments of the ray group; (ii) the number of P segments; (iii) the polarization at the source and at the receiver; (iv) the number of reflection and transmission coefficients of each type (R^{I}_{PP}, R^{I}_{PS}, R^{I}_{SP}, R^{I}_{SS}, R^{II}_{PP}, R^{II}_{PS}, R^{II}_{SP}, R^{II}_{SS}, T^{II}_{PP}, T^{II}_{PS}, T^{II}_{SP}, T^{II}_{SS}). Sequences for rays of type 1 contain the same quantities except the transmission coefficients. It is important to note that the sequence codes do not depend on time nor on the position of the receiver.

The various sequences associated with one ray group are obtained by iteration, departing from the set of sequences of the previous group; the sequences of the first ray group are used in the program for the initialization of the iterative process.

Degenerescence of rays: In a given ray group, many rays that are actually different have the same sequence of code (for example the rays of type 1 *PPPSP* and *PSPPP* have the same sequence). This phenomenon, referred to as *degenerescence*, must be taken into account in order to minimize the computation time and required memory space. Calculating ray groups of more than a few segments without taking degenerescence into account is practically impossible. The

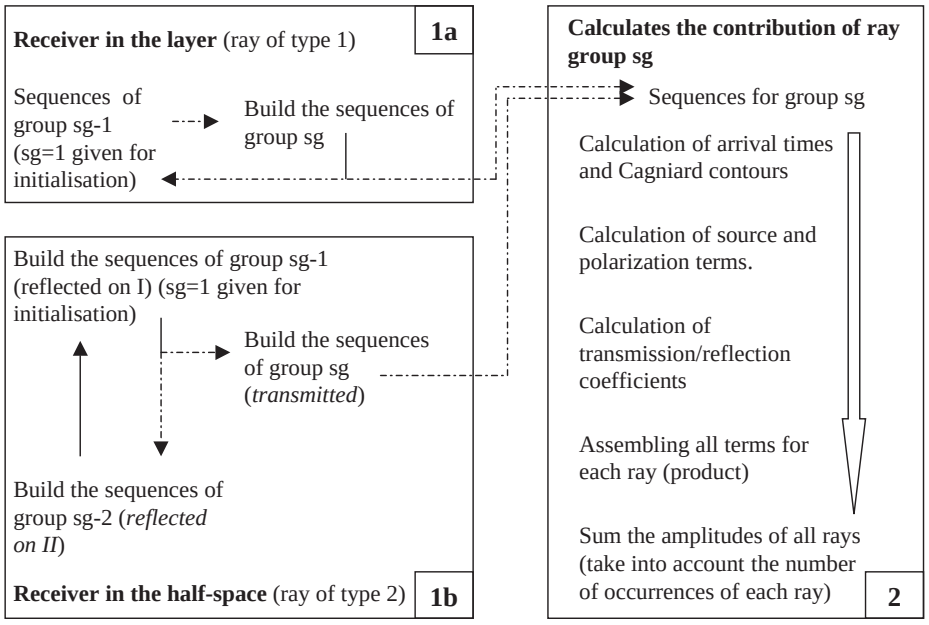

Fig. 3. Synopsis of the computer program that calculates the response as a sum of generalized ray contributions. The group number (number of segments of the rays) is denoted by sg. The discontinuous lines correspond to stages at which degenerated rays are eliminated. In boxes 1a and 1b are illustrated the iterative generation of the ray sequences. In box 2 is illustrated the kernel of the program which calculates the space-time domain contribution of a ray group.

number of degenerated rays in a group increases with the number of segments of the ray group, for instance, among the 67,108,864 (2^{26}) rays of type 1 with 26 segments, only 7232 have different sequences and actually need to be computed. The number of occurrences of a given sequence is stored together with the code of the sequence.

5.2. Program verification

Many analytical solutions available in the literature have been used to check the stress and displacement (or velocity) responses calculated by the program.

The solution of Lamb's problem (dynamic point force acting at the surface of a half-space), as given by Johnson [20] has been implemented and the results perfectly match those obtained with the authors' program. The static solutions of Lamb's problem [21, p. 412] have also been used.

It could be checked that the program properly handles the generation of rays, treatment of degenerescence and summation of ray groups by calculating the long-time (static) response of the layer to a step of force ($\phi(t) = \mathrm{H}(t)$, where $\mathrm{H}(t)$ is the Heaviside step function) with sliding contact condition at the interface and taking numerical values for the mechanical parameters of the half-space such that it can be considered as rigid in comparison with the layer. These material and loading configurations correspond to a static solution obtained by Lur'e [22]; in his calculations, Lur'e considers a *rigid* half-space and an arbitrary distributed load at the free surface. For a point force of unit amplitude normal to the free surface and a receiver on the $\mathbf{x}_3$-axis, the displacement is

$$u_3 = \frac{h}{4\pi^2\mu}\int_{-\infty}^{\infty}\int_{-\infty}^{\infty}\frac{X_2(\gamma z)}{\gamma\Delta(\gamma h)}\,\mathrm{d}\eta\,\mathrm{d}\zeta, \quad \text{where } \Delta(\gamma h) = 2h\gamma + \sinh 2h\gamma,$$
$$X_2(\gamma z) = \frac{1}{h}[\gamma h\cosh\gamma h\sinh\gamma z - \gamma z\cosh\gamma z\sinh\gamma h + 2(1-\nu)\sinh\gamma z\sinh\gamma h], \tag{31}$$

where $z = h - x_3$, $\gamma = (\eta^2 + \zeta^2)^{1/2}$ and ν is the Poisson ratio of the layer. (Note that there is a singularity in the integrand of (31) at $\gamma = 0$ that must be dealt with in the evaluation of the integral.) The long-time response of the layer is calculated with the generalized ray solution at location $x_3 = 0.015$ with $h = 0.02$ and $\rho_1 = 1750$, $c_{P,1} = 1678$, $c_{S,1} = 685$ (setting $\lambda_2 = 10\lambda_1$ and $\mu_2 = 10\mu_1$ is enough for medium 2 to be considered as rigid). Comparison with the static solution obtained with (31) is shown in Fig. 4 in a time window corresponding to the calculation of the first 20 ray groups. Both the responses with sliding and welded contact at surface II are plotted; sliding contact corresponds to the solution of Lur'e and is in agreement with the static value; the response for welded contact condition is shown for comparison.

6. Results

The numerical results presented in this section are relevant to the study of non-penetrating impact on human thorax. In the structure shown in Fig. 1, the layer and the half-space correspond to the thoracic wall and the lung, respectively. The model is used to characterize the transmission of energy in the lung, which is a biological tissue having little resistance to dynamic loadings [23]. The material parameters of the media are given in Table 1; they are such that medium 1 is "hard" in comparison with medium 2. From the viewpoint of wave propagation, the impedances of the

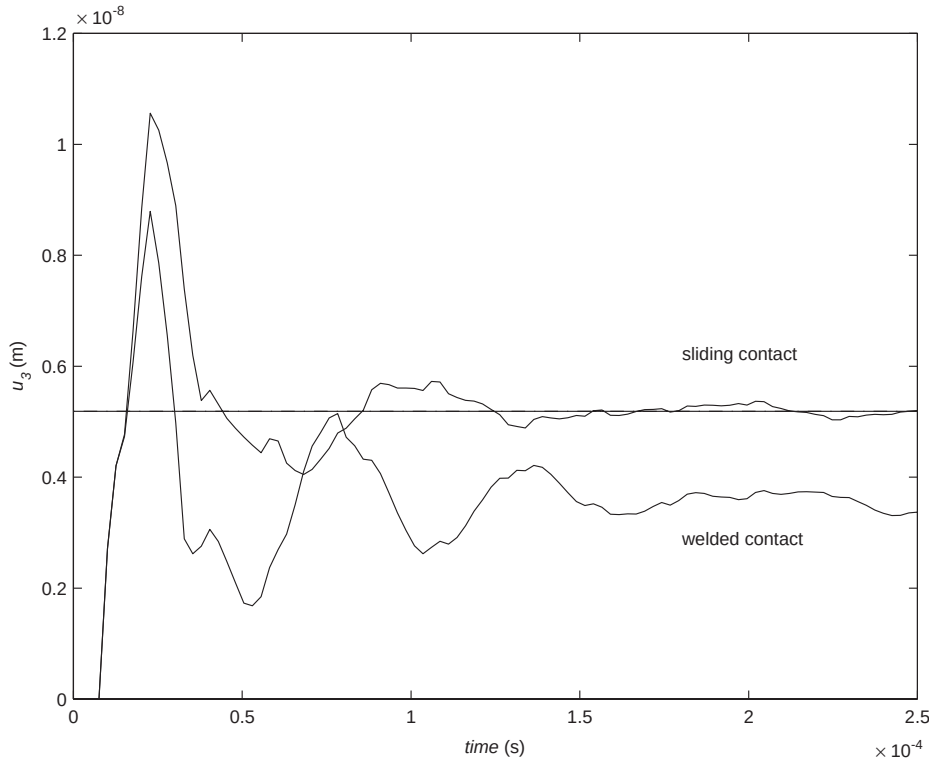

Fig. 4. Displacement $u_3(t)$ in the layer for a step of force ($\phi(t) = H(t)$) at the free surface, the half-space being rigid, for sliding and welded contact at the interface. The straight horizontal line corresponds to the static response obtained by Lur'e [22] for sliding contact.

Table 1
Material parameters and wave speeds in media 1 and 2

λ_1 (MPa)	μ_1 (MPa)	ρ_1 (kg/m^3)	c_S^1 (m/s^1)	c_P^1 (m/s^1)	λ_2 (MPa)	μ_2 (MPa)	ρ_2 (kg/m^3)	c_S^2 (m/s^1)	c_P^2 (m/s^1)
3 285	821	1 750	685	1 678	0.4	0.26	600	21	40

media are of different orders of magnitude, hence the layer and the half-space are said to be *weakly coupled*, and the typical results obtained may be valid for other weakly coupled structures. The thickness h of the layer is set to 2 cm. Both welded and sliding contact conditions at surface II were considered in the computations. (The most appropriate contact condition to model the thoracic wall-lung interface is probably sliding. Indeed, the lung and the thoracic wall are separated by a small potential space—the pleural cavity—which contains a lubricating fluid allowing the media to move easily on each other.)

Throughout this section, only receivers located on the $\mathbf{x}_3$-axis are considered, that is, $x_1 = x_2 = 0$; in the rest of this section, only the x_3-co-ordinate is specified.

The time history $\phi(t)$ of an impact is modelled by a four-point optimum Blackman window function [13] of duration T and of unit amplitude. Its second derivative is

$$\partial_{tt}\phi(t) = 0 \quad \text{for } t \leqslant 0 \text{ and } t \geqslant T, \quad \text{and} \quad \partial_{tt}\phi(t) = -(2\pi/T)^2 \sum_{n=0}^{3} b_n n^2 \cos(2\pi n t/T)$$

for $0 < t < T$, where $b_0 = 0.35869$, $b_1 = -0.48829$, $b_2 = 0.14128$ and $b_3 = -0.01168$. The amplitude of the loading is set to $\sigma_0 = -1$.

The duration of the impulse is considered with respect to the *transit time in the layer* ($h/c_{P;1} = 11.919$ μs), which is a characteristic time for the response of the structure. Figs. 5 and 6 show typical responses for various loading durations in terms of the stress σ_{33}, in the half-space at a receiver placed on the $\mathbf{x}_3$-axis at 5 mm from the interface. Both "short" pulses—of a duration of about or less than the transit time—and "long" pulses—of a duration several times the transit time—are considered. For short pulses (Fig. 5), the responses obtained with sliding or welded contact were indistinguishable. In the plots of Fig. 5, the arrival times of the waves with multiple reflections at the surfaces of the layer are manifest; the energy arriving at the receiver for a long-time after the pulse has ended. Slight differences due to the contact conditions are observed for long pulses (Fig. 6); both amplitudes and shapes are influenced (in particular, the response is shorter with sliding contact). In the plots of Fig. 6, it is seen that for loading durations of more

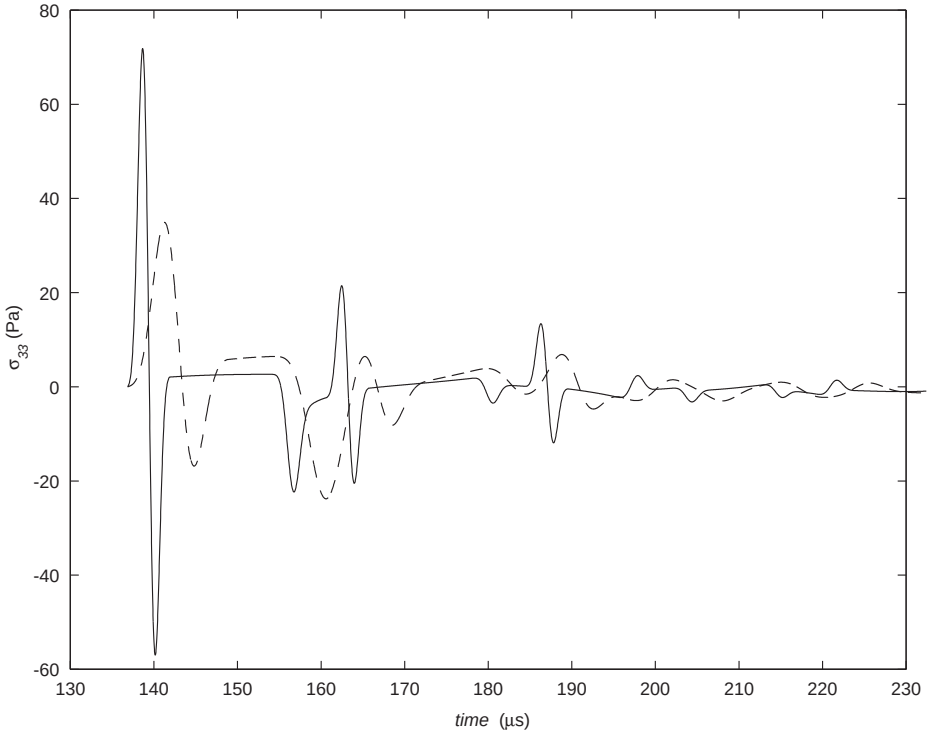

Fig. 5. Stress $\sigma_{33}(t)$ for a receiver in the half-space at 5 mm from the interface for welded contact. —, impulse duration $T = 5$ μs; - - -, $T = 11.919$ μs (equal to the transit time in the layer).

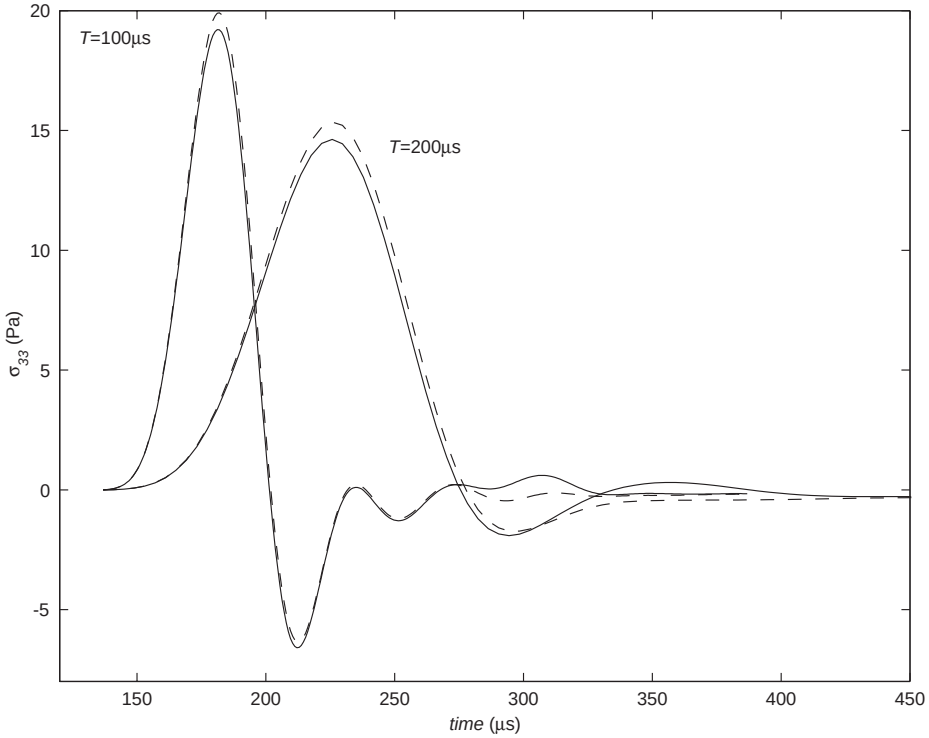

Fig. 6. Stress $\sigma_{33}(t)$ at a receiver in the half-space at 5 mm from the interface for impulse durations $T = 100$ and 200 μs. —, welded contact; - - -, sliding contact.

that 10 transit times, the wave phenomena observed in Fig. 5 are replaced by vibrations of small amplitudes. For longer loadings, the response has almost the shape of the input pulse and vibrations disappear.

Although all the responses shown in Figs. 5 and 6 correspond to a loading of unit amplitude, large discrepancies in the amplitude of the response are observed. It is seen that the shorter the loading, the greater the amplitude of the transmitted stress. In other words, the results demonstrate that a load applied slowly generates stresses of smaller amplitudes as compared to the same load applied rapidly.

Fig. 7 shows the response to a 100 μs-pulse at receivers in the half-space at various distances d from the interface; it is seen that the shape of the pulse does not change during the propagation and that the amplitude only slightly decreases. These characteristics, typical of weakly coupled bimaterial, were already reported in Ref. [14]—the low decreasing of the amplitude of the waves in medium 2 was shown to correlate with the small geometrical spreading associated with a weak curvature of the wave fronts. Plots of Fig. 7 may be compared to those of Fig. 8 which correspond to a material configuration resulting in strong mechanical coupling (the parameters of medium 2 are set to $\rho_2 = 600\ \mathrm{kg/m^3}$, $\lambda_2 = 1640$ MPa, $\mu_2 = 410$ MPa, the parameters of medium 1 are as indicated in Table 1). With this material configuration, the propagation patterns are very different to those of the weakly coupled case: the amplitude

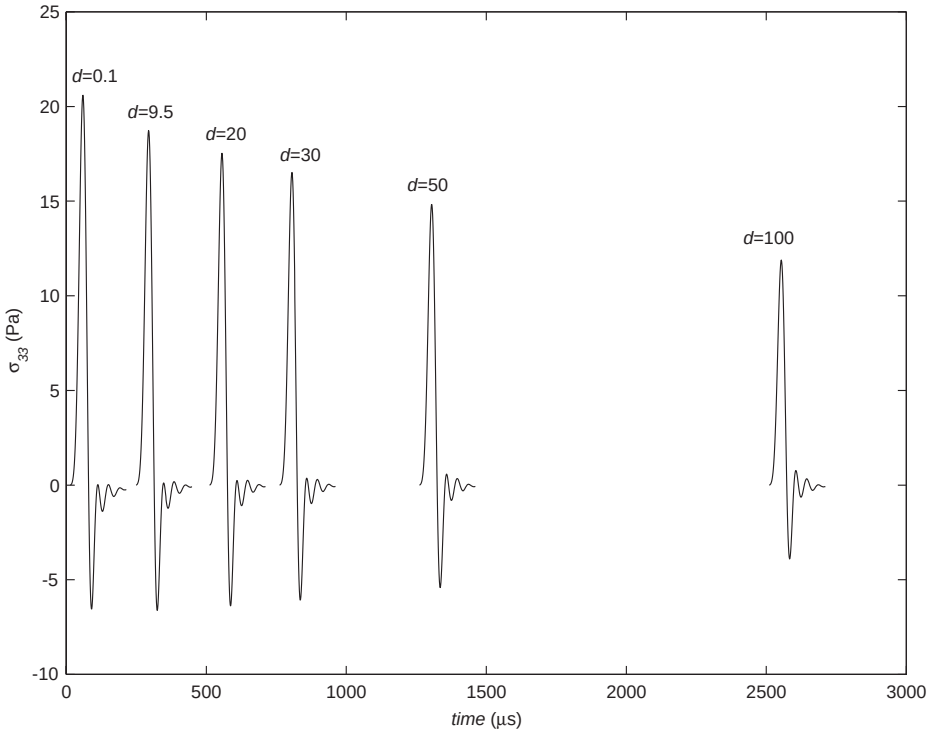

Fig. 7. Stress $\sigma_{33}(t)$ at receivers in the half-space at various distances from the interface d (in mm, indicated on the figure) for an impulse of duration $T = 100$ μs (welded interface).

of the pulse decreases rapidly with the distance from the interface, and the pulse shape changes during propagation. It is interesting to note that the amplitude at about 10 cm from the interface is of the same order of magnitude for the two material configurations—weak-coupled and strongly coupled cases—although the amplitude close to the interface is more than 50 times larger for strong coupling.

Kinematic response of the layer: As a consequence of weak coupling between the layer and the half-space, the kinematic of the layer is only slightly influenced by the presence of the half-space. In particular, as shown in Fig. 9, the kinematic of the layer under a ''long'' dynamic loading is close to that of a plate of infinite extent calculated with the classical theory of plates. The response at the epicenter of a plate for a dynamic point load excitation is calculated with [24]

$$v_3(t) = \frac{P}{8\sqrt{D\rho h}}\,\phi(t),$$

where $D = (Eh^3)/(12(1-\nu^2))$, P is the loading amplitude, E and ν are Young's modulus and the Poisson ratio of the layer, respectively. It is seen in Fig. 9 that, as could be expected, the longer the pulse, the better the correlation between the plate and layer responses.

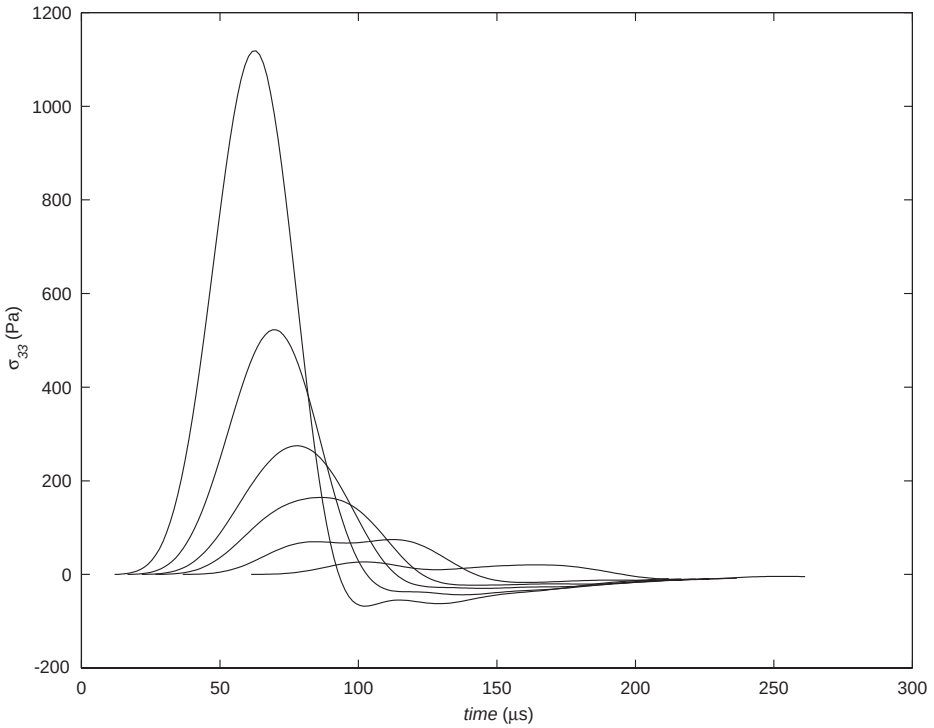

Fig. 8. Stress $\sigma_{33}(t)$ at receivers in the half-space at various distances from the interface for an impulse duration $T = 100$ μs (welded interface). The material configuration chosen offers good mechanical coupling between the layer and the half-space. The curves correspond to the same receiver locations as those indicated in Fig. 7.

7. Conclusion

In this paper a method has been presented to calculate the response of a structure made of a layer overlaying a half-space subjected to a dynamic point force applied on the free surface. The method of solution yields an exact solution of the elastodynamics problem in terms of generalized rays; however, the generalized ray solution is not obtained "by intuition" but as a result of algebraic manipulations in a Laplace–Fourier transform domain. The mathematical expression of each generalized ray contributing to the response in a given time window is derived systematically from the form of the solution. The method presented is independent of the material parameters of the layer and the half-space.

The analysis was limited to points on the axis of symmetry of the configuration ($x_1 = x_2 = 0$); in this case the time histories of velocities and stresses in the structure can be calculated with minimum use of numerical methods (in particular, the response at a point in the layer is obtained in closed form). It is thus possible to calculate the very large number of generalized rays required to obtain responses in relatively large time windows. The results presented in this paper demonstrate that exact solutions, for a tridimensional problem, can be obtained in practice with the generalized ray theory for impulses of about 30 times the characteristic time of the structure (i.e., transit time in the layer). Responses obtained by summation of about 500×10^6 generalized

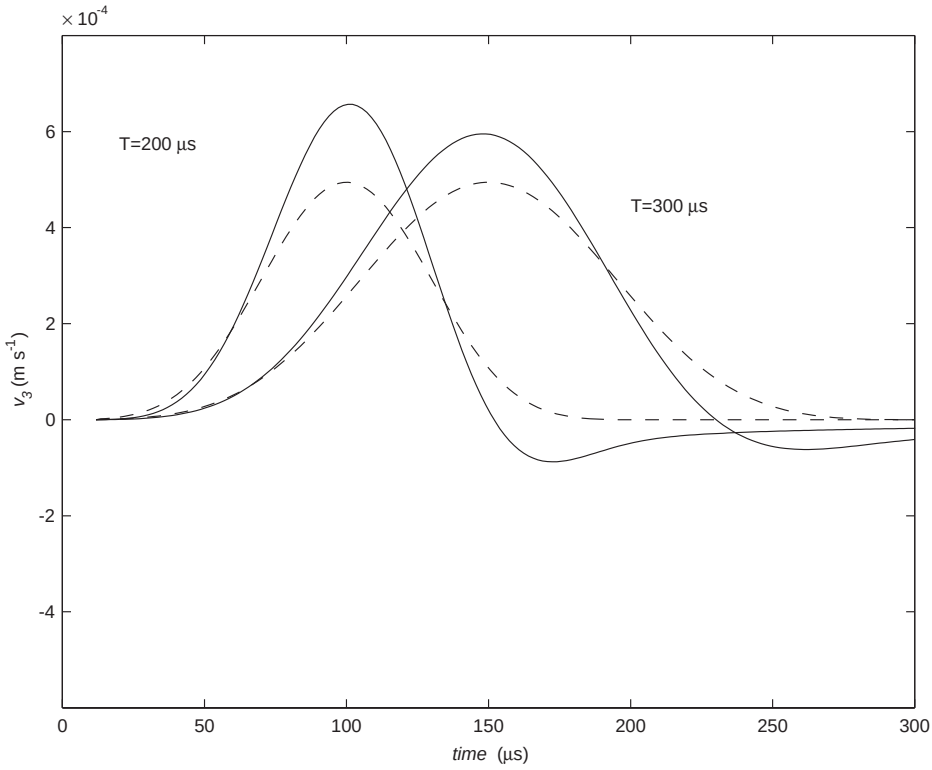

Fig. 9. Velocity $v_3(t)$ at the bottom surface of the layer for "long" loading durations $T = 200$ and 300 μs. —, generalized ray solution; - - -, solution from the classical theory of plates.

rays are presented (of course, due to degenerescence, many rays need not be explicitly computed). As an indication of the computational efforts developed, the computation time required to obtain the results presented is less than 1 h on a standard personal computer, and the responses plotted in Fig. 4 required about ninety seconds.

A practical limit arose in the computations for ray groups containing more than about 30 segments (which corresponds to loading durations of more than 30 transit times). This is due to the fact that the amplitude of each ray diverges with time (while the sum of all the rays of a given group converges), in such a way that the first rays calculated (say those of ray group one) have very large amplitudes at large times when the rays of higher order groups arrive at the receiver: When these large amplitudes are summed, numerical errors are induced.

Concerning the biomechanical application, the results contribute to elucidate the response of the thorax to loadings of various durations. Typical impacts of "high"-velocity projectiles result in loading durations in range 1–500 μs. The method and the associated computer program make it possible to determine, for arbitrary loading history and a wide range of impulse durations: (i) the maximum amplitudes of velocities and stresses transmitted; (ii) the time elapsed before the structure returns at rest; (iii) the effects of the contact condition (sliding or welded) assumed at the thoracic wall-lung interface.

Acknowledgements

The authors thank the "Délégation Générale pour l'Armement" of the Minister of Defense of France for supporting this work.

Appendix A. Reflection and transmission coefficients

The explicit expressions of the coefficients are obtained through the derivation of the solution in the transform domain presented in Section 3. They are equivalent to the well-known coefficients for plane waves.

Reflection coefficients at surface I (*free surface*):

$$R_{PP} = R_{SS} = (s_3^{P;1} s_3^{S;1} S^2 - \chi_1^2)\Delta_{R;1}^{-1},$$

$$R_{PS} = (-2c_{P;1} s_{S;1} s_3^{P;1} \chi_1 S)\Delta_{R;1}^{-1}; \quad R_{SP} = (2s_{P;1} c_{S;1} s_3^{S;1} \chi_1 S)\Delta_{R;1}^{-1}, \tag{A.1}$$

where $\Delta_{R;1} = s_3^{P;1} s_{3;1}^{S} S^2 + \chi_1^2$ is the Rayleigh wave denominator.

Reflection and transmission coefficients at interface II (*welded contact*):

$$R_{PP} = (F(bs_3^{P;1} - cs_3^{P;2}) - H(a + ds_3^{P;1} s_3^{S;2})S^2)D^{-1},$$

$$R_{PS} = (-2s_3^{P;1}(ab + cds_3^{P;2} s_3^{S;2} S c_{P;1})(c_{S;1} D)^{-1},$$

$$R_{SP} = (2s_3^{S;1}(ab + cds_3^{P;2} s_3^{S;2} S c_{S;1})(c_{P;1} D)^{-1},$$

$$R_{SS} = (E(bs_3^{S;1} - cs_3^{S;2}) - G(a + ds_3^{P;2} s_3^{S;1})S^2)D^{-1}, \tag{A.2}$$

$$T_{PP} = (2\rho_1 s_3^{P;1} F c_{P;1})(D c_{P;2})^{-1}; \quad T_{PS} = (-2\rho_1 s_3^{P;1} H S c_{P;1})(D c_{S;2})^{-1},$$

$$T_{SP} = (2\rho_1 s_3^{S;1} G S c_{S;1})(D c_{P;2})^{-1}; \quad T_{SS} = (2\rho_1 s_3^{S;1} E c_{S;1})(D c_{S;2})^{-1}, \tag{A.3}$$

where

$$a = \rho_2(1 - 2c_{S;2}^2 S^2) - \rho_1(1 - 2c_{S;1}^2 S^2); \quad b = \rho_2(1 - 2c_{S;2}^2 S^2) + 2\rho_1 c_{S;1}^2 S^2,$$

$$c = \rho_1(1 - 2c_{S;1}^2 S^2) + 2\rho_2 c_{S;2}^2 S^2; \quad d = 2(\rho_2 c_{S;2}^2 - \rho_1 c_{S;1}^2),$$

$$E = bs_3^{P;1} + cs_3^{P;2}; \quad F = bs_3^{S;1} + cs_3^{S;2},$$

$$G = a - ds_3^{P;1} s_3^{S;2}; \quad H = a - ds_3^{P;2} s_3^{S;1}; \quad D = EF + GHS^2.$$

Reflection and transmission coefficients at interface II (frictionless sliding contact) [25]:

$$\begin{aligned}
&R_{PP} = (E_2F_1 + F_2G_1)H^{-1}; \quad R_{SP} = (-4F_2\mu_1 c_{S;1} s_3^{S;1}\chi_1)(Hc_{P;1})^{-1},\\
&R_{PS} = (4F_2\mu_1 c_{P;1} s_3^{P;1}\chi_1)(Hc_{S;1})^{-1}; \quad R_{SS} = (-E_2F_1 + F_2G_1)H^{-1},\\
&T_{PP} = (4F_1\mu_1 c_{P;1}\chi_1\chi_2 S^{-1})(Hc_{P;2})^{-1}; \quad T_{SP} = (4F_1\mu_1 c_{S;1} s_3^{S;1}\chi_2)(Hc_{P;2})^{-1},\\
&T_{PS} = (4F_1\mu_1 c_{P;1}\chi_1 s_3^{P;2})(Hc_{S;2})^{-1}; \quad T_{SS} = (4F_1\mu_1 c_{S;1} s_3^{S;1} s_3^{P;2} S)(Hc_{S;2})^{-1},
\end{aligned} \tag{A.4}$$

where

$$\begin{aligned}
&E_m = 2\mu_m S^{-1}\Delta_{R;m}; \quad F_m = 0.5S^{-1} s_3^{P;m} s_{S;m}^2,\\
&G_m = 2\mu_m(s_3^{P;m} s_3^{S;m} S - \chi_m^2 S^{-1}); \quad H = (F_1E_2 + F_2E_1),
\end{aligned}$$

where

$$\Delta_{R;m} = s_3^{P;m} s_3^{S;m} S^2 + \chi_m^2, \ m = 1, 2.$$

Appendix B. Cagniard–de Hoop contours

Cagniard–de Hoop contour in the layer: Variable S that defines the Cagniard–de Hoop contour for a receiver placed on the $\mathbf{x}_3$-axis is the solution of an equation of the form

$$\tau = g(S) = \sum s_3^{P,S;1} h + s_3^{P,S;1} x_3. \tag{B.1}$$

The solution for (B.1) was obtained in Ref. [14] and is reproduced below. Rewriting (B.1) under the form

$$\tau = (mh \pm x_3\delta_{\beta P}) s_3^{P;1} + (nh \pm x_3\delta_{\beta S}) s_3^{S;1},$$

where $\beta = P$ or S is the polarization associated with the last ray segment and $\delta_{SS} = \delta_{PP} = 1$, $\delta_{SP} = \delta_{PS} = 0$; m and n are, respectively, the number of P and S ray segments (not counting the last segment). Denoting $H_P = (mh \pm x_3\delta_{\beta P})$ and $H_S = (nh \pm x_3\delta_{\beta S})$, the arrival time T_a of the ray is

$$T_a = H_P s_{P;1} + H_S s_{S;1}.$$

The Cagniard–de Hoop contour is given by

$$S = \pm\sqrt{s_{S;2}^2 - Y^2},$$

where, if $H_P \neq H_S$

$$Y = \frac{\tau H_S - H_P\sqrt{\Delta}}{H_S^2 - H_P^2} \quad \text{with } \Delta = [(H_P s_{S;2} + H_S s_{P;1})^2 - T_a^2 + \tau^2],$$

and if $H_P = H_S = H$

$$Y = [2H^2 s_{S;2}(s_{P;1} + s_{S;2}) + \tau^2 - T_a^2](2\tau H)^{-1}.$$

Cagniard–de Hoop contour in the half-space: Variable S that defines the Cagniard–de Hoop contour for a receiver placed on the $\mathbf{x}_3$-axis is the solution of an equation of the form

$$\tau = g(S) = \sum s_3^{P,S;1} h + s_3^{P,S;2}(x_3 - h),$$

or, by using the same notation as for the contour in the layer,

$$\tau = mhs_3^{P;1} + nhs_3^{S;1} + (h - x_3)s_3^{P,S;2}. \tag{B.2}$$

Unless $m + n = 1$, the solution S of (B.2) must be calculated with a numerical method.

References

[1] A.G. Mencher, Epicentral displacement caused by elastic waves in an infinite slab, *Journal of Applied Physics* 24 (1953) 1240–1246.

[2] T.W. Spencer, The method of generalized reflection and transmission coefficients, *Geophysics* 25 (1960) 625–641.

[3] Y. Pao, R. Gajewski, The generalized ray theory and transient response of layered elastic solids, in: W.P. Mason, R.N. Thurston (Eds.), *Physical Acoustics XIII*, Academic, New York, pp. 183–265.

[4] L. Cagniard, *Reflection and Refraction of Progressive Seismic Waves*, Mc-Graw Hill, New York, 1962 (Translation and revision by E.A. Flinn, C.H. Dix, of L. Cagniard, Réflexion et Réfraction des Ondes Séismiques Progressives, Gauthier-Villars, Paris, 1939).

[5] A.T. de Hoop, A modification of Cagniard's method for solving seismic pulse problems, *Applied Scientific Research* 8 (1960) 349–356.

[6] L. Knopoff, Surface motions of a thick plate, *Journal of Applied Physics* 29 (1958) 661–670.

[7] N. Davids, Transient analysis of stress-wave penetration in plates, *Journal of Applied Mechanics* 26 (1959) 651–660.

[8] J. Miklowitz, Transient compressional waves in an infinite elastic plate or elastic layer overlying a rigid half-space, *Journal of Applied Mechanics* 29 (1962) 53–60.

[9] R.L. Weaver, Y.-H. Pao, Axisymmetric elastic waves excited by a point source in a plate, *Journal of Applied Mechanics* 49 (1982) 821–836.

[10] N. Davids, W. Lawhead, Transient analysis of oblique impact on plates, *Journal of the Mechanics and Physics and Solids* 13 (1965) 199–212.

[11] A.N. Ceranoglu, Y.H. Pao, Propagation of elastic pulses and acoustic emission in a plate, *Journal of Applied Mechanics* 48 (1981) 125–147.

[12] K. Aki, P.G. Richard, *Quantitative Seismology: Theory and Methods*, Freeman, San Francisco, CA, 1980.

[13] J.H.M.T. van der Hijden, *Propagation of Transient Elastic Waves in Stratified Anisotropic Media*, Vol. 32, Springer, New York, 1987.

[14] Q. Grimal, S. Naïli, A. Watzky, A study of transient elastic wave propagation in a bimaterial modeling the thorax, *International Journal of Solids and Structures* 39 (2002) 5345–5369.

[15] C.C. Ma, G.S. Lee, Theoretical analysis, numerical calculation and experimental measurement of transient elastic waves in strips subjected to dynamic loadings, *International Journal of Solids and Structures* 36 (1999) 3541–3564.

[16] C.C. Ma, G.S. Lee, Transient elastic waves propagating in a multi-layered medium subjected to in-plane dynamic loadings. II. Numerical calculation and experimental measurement, *Proceedings of the Royal Society of London Series A* 456 (2000) 1375–1396.

[17] G.S. Lee, C.C. Ma, Transient elastic waves propagating in a multi-layered medium subjected to in-plane dynamic loadings. I. Theory, *Proceedings of the Royal Society of London Series A* 456 (2000) 1355–1374.

[18] X.Y. Su, J.Y. Tian, Y.H. Pao, Application of the reverberation-ray matrix to the propagation of elastic waves in a layered solid, *International Journal of Solids and Structures* 39 (2002) 5447–5463.

[19] Q. Grimal, S. Naïli, A. Watzky, Transient elastic wave propagation in a spherically symmetric bimaterial medium modeling the thorax, *International Journal of Solids and Structures* 39 (2002) 6103–6120.

[20] L.R. Johnson, Green's function for Lamb's problem, *Geophysical Journal of the Royal Astronomical Society* 37 (1974) 99–131.

[21] D. François, A. Pineau, A. Zaoui, *Comportement Mécanique des Matériaux*; *Viscoplasticité*, *Endommagement*, *Mécanique de la Rupture*, *Mécanique du Contact*, Hermès, Paris, 1993.

[22] A.I. Lur'e, *Three-dimensional problems of the theory of elasticity*, Wiley, New York, 1964 (Translation; original work published in Russian).
[23] Y.C. Fung, *Biomechanics: Motion, Flow, Stress, and Growth*, Springer, New York, 1990.
[24] M.A. Medick, On classical plate theory and wave propagation, *Journal of Applied Mechanics* 28 (1961) 223–228.
[25] Q. Grimal, S. Naïli, A. Watzky, On the transmission of transient elasto-dynamic waves at a sliding contact interface; application to a weakly coupled bimaterial, *International Journal of Solids and Structures*, in press.